THERMAL AND CATALYTIC SLOW PYROLYSIS OF LIGNOCELLULOSIC OIL PALM WASTES USING ZEOLITE AND HYDROXYAPATITE BASED CATALYSTS

By

Kabir Garba

Thesis submitted in fulfilment of the

requirement for the degree of

Doctor of Philosophy

July 2018

ACKNOWLEDMENT

Many individuals contributed in this research, I am obliged to all of them. Foremost, I'm grateful to main supervisor, Prof. Dr. Bassim H. Hammed, without whose guidance and advice this study would not be what it is. His patience, support and extraordinary expertise have enlightened me out of many bottlenecks on many times while the entire study, despite the endless support and help that I have received. I am also grateful to Dr. Azam Taufik Mohd Din for serving as Co-supervisor and for his invaluable suggestions and help.

I am thankful to the Universiti Sains Malaysia and the academic staff members of the School of Chemical Engineering for rendering the conducive environment throughout my postgraduate studies. In addition, I am grateful to laboratory technicians of the School for their commitment during the study. Especially to Mohamed Faiza Ismail, Muhammad Ismail Abu Talib, Nur'ain Natasya Shaari, Muhammad Arif Mat Husin, Mohd Roqib Rashidi, Noraswani Muhamad, Mohd Rasydan Omar, Latiffah Abdul Latif. I wish to express my gratitude to members of Reaction Engineering and Adsorption Group (READ) for their help and inspiring collaborations, especially to Dr. Waheed Khanday, Ali Lawal Yaumi, Dr. Patrick U Okoye, Norlinda Nasuha, Yee Ling Tan, Fatma Marrackchi and Hamizura Hassan.

I am endlessly indebted to my parents Abubakar Umar and Hau'wa Umar, and my grandmother Khadijah Umar for the support and encouragement through this path to success. Finally, I devote this work to my wife Salamatu and my children Al-meen, Khadija, Hauwa and Hameeda whose undaunted sacrifice and support made this work successful.

Kabir Garba
USM Engineering Campus,
School of Chemical Engineering, April 2018

TABLE OF CONTENTS

	Page
ACKNOWLEDMENT	**ii**
TABLE OF CONTENTS	**iii**
LIST OF TABLES	**v**
LIST OF FIGURES	**viii**
LIST OF SYMBOLS	**xi**
LIST OF ABBREVIATIONS	**xii**
ABSTRAK	**xiv**
ABSTRACT	**xvi**
CHAPTER ONE INTRODUCTION	**1**
1.1 Background	1
1.2 Problem statement	5
1.3 Objectives of the study	6
1.4 Scope of the study	6
1.5 Thesis organization	7
CHAPTER TWO LITERATURE REVIEW	**9**
2.1 Lignocellulosic biomass	9
2.1.1 Types and availability of lignocellulosic biomass wastes	9
2.1.2 Composition of lignocellulosic biomass	10
2.1.3 Structure of lignocellulosic biomass	12
2.1.4 Lignocellulose biomass proximate and ultimate compositions	14
2.2 Pyrolysis of lignocellulose biomass	16
2.2.1 Advantages of pyrolysis	16
2.2.2 Pyrolysis technology	17
2.2.3 Thermal pyrolysis of lignocellulosic biomass	19
2.2.4 Mechanisms of pyrolysis of lignocellulosic biomass	21
2.2.5 Effect of operating conditions on biomass pyrolysis	25
2.2.6 Studies of thermal pyrolysis of lignocellulosic biomass	28
2.2.7 Catalytic pyrolysis of lignocellulosic biomass	30
2.2.8 Catalyst for lignocellulosic biomass pyrolysis	35
2.3 Classification of adsorption isotherms	48
2.3.1 Physisorption isotherms	48
2.3.2 Adsorption hysteresis	49
2.4 Kinetics of thermal and catalytic biomass pyrolysis by thermogravimetry	50
2.5 Summary	58
CHAPTER THREE MATERIALS AND METHODS	**59**

3.1 Introduction 59
3.2 Experimental plan 59
3.3 Materials and chemicals 61
3.3.1 Lignocellulose oil palm wastes (LOPW) 61
3.3.2 Electric arc furnace slag (EAFS) 61
3.4 Description of equipment 64
3.4.1 Description of the pyrolysis fixed-bed reactor set-up 64
3.5 LOPW, catalyst and product characterizations 66
3.5.2 Catalysts characterizations 68
3.5.3 Description of instruments for bio-oil characterizations 71
3.6 Experimental procedures 72
3.6.1 Determination of LOPW chemical compositions 72
3.6.2 Synthesis of Faujasite-SL and hydroxyapatite-zeolite catalysts 73
3.6.3 Thermal and catalytic slow-pyrolysis of LOPW 76

CHAPTER FOUR RESULTS AND DICUSSION 78
4.1 Introduction 78
4.2 Thermal pyrolysis of lignocellulosic oil palm wastes (LOPW). 79
4.2.1 Characterizations of LOPW 79
4.2.2 Parametric studies of thermal pyrolysis of LOPW 83
4.3 Characterization of bio-oils from LOPW pyrolysis 89
4.3.1 Ultimate analysis of bio-oils (LOPW-oils) 89
4.3.2 Fourier transform infrared (FTIR) of LOPW-oils 91
4.3.3 Chromatograms of LOPW-oils 92
4.3.4 Characterization of LOPW-chars 104
4.4 Activity of FAU-SL and HAPAZ-based catalysts in OPMF pyrolysis 106
4.4.1 Characterization of FAU-SL, HAPAZ and Fe/HAPAZ catalysts 107
4.4.2 Pyrolysis of OPMF over FAU-SL and HAPAZ-based catalysts 118
4.4.3 Effects of FAU-SL and HAPAZ based catalysts on OPMF-oils 139
4.4.4 LOPW pyrolysis over Fe/HAPAZ catalyst 145
4.4.5 Gas composition of OPMF pyrolysis over FAU-SL and HAPAZ catalysts 152
4.5 Thermogravimetry and kinetics of LOPW pyrolysis 154
4.6 Characteristics parameters for LOPW thermal and catalytic pyrolysis. 169

CHAPTER FIVE ONCLUSIONS AND RECOMMENDATIONS 172
5.1 Conclusions 172
5.2 Recommendations on future work 174
REFERENCES 175
APPENDICES
LIST OF PUBLICATIONS

LIST OF TABLES

		Page
Table 2.1	Chemical compositions of lignocellulosic biomass.	11
Table 2.3	Proximate and ultimate compositions of lignocellulosic biomass.	15
Table 2.3	Pyrolysis conditions and product distributions.	17
Table 2.4	Compounds from primary decomposition of lignocellulosic biomass by pyrolysis.	24
Table 2.5	Summary of catalysts used in domain studies of biomass pyrolysis to high-grade bio-oil.	47
Table 2.6	The kinetics models of Coats-Redfern's method.	54
Table 2.7	Kinetics of thermal and catalytic pyrolysis of biomass by thermogravimetry.	56
Table 3.1	List of materials and chemicals.	62
Table 3.2	List of equipments used in the catalyst synthesis.	63
Table 4.1	Characteristics of lignocellulosic oil palm wastes (LOPW).	80
Table 4.2	Characteristics of LOPW-oils (temperature = 550 °C, heating rate = 10 °C/min, and N_2 flow rate = 200 mL/min).	90
Table 4.3	Chromatographic composition of OPMF-oil (temperature = 550 °C, heating rate = 10 °C/min, and N_2 flow rate = 200 mL/min).	96
Table 4.4	Chromatographic composition of PF-oil (temperature = 550 °C, heating rate = 10 °C/min, and N_2 flow rate = 200 mL/min).	98
Table 4.5	Chromatographic composition of EFB-oil (temperature = 550 °C, heating rate = 10 °C/min, and N_2 flow rate = 200 mL/min).	100

Page

Table 4.6	Chromatographic composition of PKS-oil (temperature = 550 °C, heating rate = 10 °C/min, and N_2 flow rate = 200 mL/min).	102
Table 4.7	Characteristics of LOPW-oils (temperature = 550 °C, heating rate = 10 °C/min, and N_2 flow rate = 200 mL/min).	105
Table 4.8	Textural characteristics of the HAPAZ, FAU-SL, FAU-SL/Mg, FAU-SL/Zn and Fe/HAPAZ catalysts.	112
Table 4.9	Chromatographic compositions of bio-oil from the OPMF pyrolysis over HAPAZ catalyst (N_2 flow rate = 200 mL/min, catalyst loading = 0.5 g).	129
Table 4.10	Chromatographic compositions of bio-oil from OPMF pyrolysis over FAU-SL (temperature = 550 °C, N_2 flow rate = 200 mL/min, catalyst loading = 0.5 g).	132
Table 4.11	Chromatographic composition of bio-oil from OPMF pyrolysis over FAU-SL and FAU-SL/MgO catalysts (temperature = 550 °C, N_2 flow rate = 200 mL/min, catalyst loading = 0.5 g).	133
Table 4.12	Chromatographic compositions of bio-oils from the pyrolysis of OPMF over Fe/HAPAZ catalyst (N_2 flow rate = 200 mL/min, catalyst loading = 0.5 g).	135
Table 4.13	Chromatographic compositions of bio-oil from the pyrolysis of OPMF over zeolite hydroxyapatite catalysts at pyrolysis temperature = 500 ºC, N_2 flow rate = 200 mL/min, catalyst loading = 0.5 g).	142
Table 4.14	Chromatographic compositions of bio-oil from the LOPW pyrolysis catalysed with Fe/HAPAZ catalyst (N_2 flow rate = 200 mL/min, catalyst loading = 0.5 g).	148
Table 4.15	Weight loss for the different stages of LOPW thermal and catalytic pyrolysis.	159
Table 4.16	Kinetic parameters of the LOPW pyrolysis from the chemical reaction models'.	164

Page

Table 4.17	Kinetic parameters of the LOPW pyrolysis from the diffusion kinetics of the CR methods.	165
Table 4.18	Kinetic parameters of the LOPW pyrolysis from the power law kinetics of the CR methods.	166
Table 4.19	Kinetic parameters of the LOPW pyrolysis from the Avarami-Erofe'ev kinetics of the CR methods.	167
Table 4.20	Kinetic parameters of the LOPW pyrolysis from the geometrical contraction kinetics of the CR methods.	168
Table 4.21	Characteristics parameters and characteristic index D for thermal and catalytic pyrolysis of LOPW at heating rate 10 ^{o}C/min.	170

LIST OF FIGURES

		Page
Figure 2.1	Typical structures of (a) cellulose, hemicellulose (xylan) and (c) lignin of lignocellulosic biomass.	13
Figure 2.2	Representative compounds of vapor from lignocellulosic biomass pyrolysis.	20
Figure 2.3	Reaction pathways cellulose decomposition by pyrolysis.	22
Figure 2.4	Reaction pathways for lignin decomposition by pyrolysis.	23
Figure 2.5	Schematic of catalytic pyrolysis process for lignocellulosic biomass conversion.	31
Figure 2.6	Reaction pathways of catalytic pyrolysis of lignocellulosic biomass.	33
Figure 2.7	Representative reactions for synthesis of aromatics from hollocellulose over ZSM-5.	37
Figure 2.8	Secondary reactions for synthesis of aromatics from CPV over ZSM-5.	38
Figure 2.9	A representative lignin pyrolysis reaction over a typical base catalyst	43
Figure 2.10	Types of physisorption isotherms and (b) Types of hysteresis	48
Figure 3.1	Experimental flow diagram for thermal and catalytic pyrolysis of LOPW.	60
Figure 3.2	(a) Images and (b) schematic of the pyrolysis fixed-bed experimental rig.	65
Figure 4.1	FTIR spectra of lignocellulosic oil palm wastes (LOPW).	82
Figure 4.2	Effect of N_2 flow rate on products distribution from the pyrolysis of (a) OPMF, (b) PF, (c) EFB-oil and (d) PKS (temperature = 550 °C, heating rate = 10 °C/min).	84

Figure 4.3	Product distributions from the pyrolysis of (a) OPMF, (b) PF, (c) EFB and (d) PKS at different pyrolysis temperatures (conditions: reaction time of 15 min, and N_2 flow rate of 200 mL/min).	87
Figure 4.4	FTIR spectra of bio-oils from slow pyrolysis of LOPW (conditions: temperature = 550 °C, heating rate = 10 °C/min, and N_2 flow rate = 200 mL/min).	91
Figure 4.5	Relative abundance and categories of the tentative compounds of (a) OPMF-oil and (b) PF-oil, (c) PKS-oil and (d) EFB-oil (conditions: temperature = 550 °C, heating rate = 10 °C/min, and N_2 flow rate = 200 mL/min).	93
Figure 4.6	XRD patterns of (a) HAPAZ (b) FAU-SL (c) Fe/HAPAZ calcined at 450 ºC.	108
Figure 4.7	N_2 adsorption-desorption isotherm and pore size distribution curves of the (a) HAPAZ, (b) FAU-SL, (c) FAU-SL/Mg and Zn, and (d) Fe/HAPAZ catalyst.	110
Figure 4.8	EDX spectrum and elemental composition of (a) HAPAZ, (b) FAU-SL, (c) FAU-SL/Mg, (d) FAU-SL/Zn and (e) Fe-HAPAZ catalysts calcined at 450 ºC.	114
Figure 4.9	SEM images of (a) HAPAZ, (b) FAU-SL, FAU-SL, (c) FAU-SL/Mg, FAU-SL/Zn and (e) Fe/HAPAZ catalysts calcined at 450 ºC (10 000 magnification).	117
Figure 4.10	Product yields of OPMF pyrolysis over (a) HAPAZ, (b) FAU-SL and (c) Fe/HAPAZ at different loading (OPMF= 5.0 g, Pyrolysis temperature = 550 ºC, N_2 flow rate =200 mL/min).	119
Figure 4.11	Product yields of the pyrolysis pf OPMF over (a) HAPAZ, (b) FAU-SL and (c) Fe/HAPAZ at different pyrolysis temperature (OPMF= 5.0 g, catalyst load = 0.5 g, N_2 flow rate =200 mL/min).	121
Figure 4.12	Relative abundance of compounds from OPMF pyrolysis over (a) HAPAZ, (b) FAU-SL, FAU-SL, (c) FAU-SL/Mg, FAU-SL/Zn and (e) Fe/HAPAZ catalysts at different temperatures, catalyst loading = 0.5 g and N2 flow rate = 200 mL/min.	124

Page

Figure 4.13 Relative abundance of compounds from OPMF pyrolysis over FAU-SL/MgO and FAU-SL/ZnO catalysts at pyrolysis temperature = 550 °C, catalyst loading = 0.5 g and N_2 flow rate = 200 mL/min. 127

Figure 4.14 Relative abundance of compounds in bio-oils from OPMF pyrolysis over FAU-SL and HAPAZ-based catalysts at pyrolysis temperature = 500 °C, catalyst loading = 0.5 g and N_2 flow rate = 200 mL/min. 139

Figure 4.15 Relative abundance of compounds in bio-oils from LOPW pyrolysis over Fe/HAPAZ catalyst (Pyrolysis temperature = 550 °C, catalyst loading = 0.5 g, N_2 flow rate = 200 mL/min). 145

Figure 4.16 Composition profiles of NCG (N_2 free basis) from OPMF pyrolysis over (a) HAPAZ, (b) FAU-SL, and (c) Fe/HAPAZ catalysts (OPMF= 5.0 g, catalyst load = 0.5 g, N_2 flow rate =200 mL/min). 153

Figure 4.17 TG curves of thermal pyrolysis and catalytic pyrolysis (LOPW:Catalyst mass ratio = 4:1; N_2=20 mL/min; heating rate of 10 oC/min). 155

Figure 4.18 DTG curves of thermal and catalytic pyrolysis of LOPW (LOPW:Catalyst mass ratio = 4:1; N_2=20 mL/min; heating rate of 10 °C/min). 157

LIST OF SYMBOLS

Symbol	Description	Unit
α	Degree of conversion	-
T	Absolute temperature	K
t	Time of decomposition	min
w	Percentage weight loss	%
E_a	Activation energy	kJ/mol
A	Arrhenius constant	min^{-1}
R	Gas constant	J/mol. K
β	Heating rate	^oC/min
T_i	Initial decomposition temperature	^oC
T_p	Peak temperature of each phase	^oC
R_p	Maximum weight loss rate of each phase	%/min
T_f	Terminal/Final decomposition temperature (^oC)	^oC
t_f	Terminal/Final decomposition	min
$\Delta T_{1/2}$	Temperature interval at half value of $-R_p$ of each phase	^oC
M_r	Residual weight after pyrolysis experiment	%
TG_{total}	Total mass loss	wt%
R_v	Average pyrolysis rate	(% /min)
D	Comprehensive devolatilization index	$(\%^2{}^oC^{-3}min^{-2})$
M_∞	Pyrolysis weight loss	wt%
HHV	High heating value	MJ/kg
λ	Wavelength	cm

LIST OF ABBREVIATIONS

Symbol	Description
AAE	Alkali and alkaline earth metals
ASTM	American Society for Testing and Materials
BET	Brunauer–Emmett–Teller
BJH	Barrett–Joyner–Halenda
BOFS	Basic oxygen furnace slag
CBO	Crude bio-oil
CPV	Crude pyrolysis vapor
CR	Coats-Redfern methods
CSP	Catalytic slow pyrolysis
D	Devolatilization index
DEAM	Distributed activation energy model
DTG	Derivative thermogravimetry
EAFS	Electric arc furnace slag
EDX	Energy dispersive X-ray
EFB	Empty fruit brunches
FTIR	Fourier transform infra-red
FWO	Flynn-Wall-Ozawa
GC-MS	Gas-chromatography and Mass spectrometer
GC-TCD	Gas-chromatography- Thermal conductivity detector
HAP	Hydroxyapatite
HAPAZ	Hydroxyapatite-zeoilite
KAS	Kissinger-Akahira-Sunose

KBr	Potassium bromide
LOPW	Lignocellulosic oil palm wastes
NCG	Non-condensable gas
NTIS	National Institute of Standards and Technology library
OPMF	Oil palm mesocarp fiber
PF	Palm frond
PKS	Palm kernel shell
Py-GC-MS	Pyrolysis- Gas-chromatography and Mass spectrometer
SEM	Scanning electron microscopy
TG	Thermogravimetry
TGA	Thermogravimetric analysis
XRD	X-ray diffraction

PIROLISIS PERLAHAN HABA DAN BERMANGKIN KE ATAS SISA LIGNOSELULOSA SAWIT MENGGUNAKAN PEMANGKIN BERASASKAN ZEOLIT DAN HIDROKSIAPATIT

ABSTRAK

Kebimbangan berkaitan dengan sisa industri merangsang pengeluaran minyak-bio yang berkualiti dari pirolisis sisa kelapa sawit lignoselulosa dengan mangkin mesoliang boleh jaya terbitan daripada sisa keluli sanga. Kajian ini menyiasat pirolisis haba dan bermangkin bagi LOPW ke atas pemangkin yang berasaskan zeolit dan zeolit-hidroksiapatit untuk menghasilkan minyak-bio yang berkualiti di dalam reaktor lapisan tetap pemanasan perlahan. Juga, kinetik pirolisis haba dan pemangkin LOPW disiasat dengan menggunakan kaedah Coats-Redfern. Reaktor dikekalkan pada suhu pirolisis 450-600 °C, kadar aliran N_2 200 mL/min, kadar pemanasan 10 °C/min dan 0.5-2.5 g beban pemangkin digunakan untuk pirolisis bermangkin. Pirolisis bermangkin dilakukan atas zeolit dan zeolit-hidroksiapatit, sebagai pemangkin yang disediakan dari arka elektrik jermang relau. Ciri-ciri tekstur BET mencadangkan bahawa pemangkin adalah hierarki dan sangat bermesoliang dengan purata diameter liang antara 23-25 nm. Pemangkin zeolit mempunyai struktur kristal yang konsisten dengan zeolit Faujasite-Ca, berdasarkan pengesahan oleh analisis XRD. Manakala Faujasite-Ca zeolit dan kumin hablur hidroksiapatit membentuk struktur rencam pemangkin hidroksiapatit-zeolit. Pirolisis haba menghasilkan minyak-bio mentah (CBO) pada kadar maksimum 40-47 wt% di bawah suhu pirolisis 500-550 °C, sedangkan pirolisis bermangkin ke atas 0.5 g pemangkin ialah 40-47 wt%. CBO mempunyai nilai pemanasan yang tinggi dari 21-24.68 MJ/kg lebih tinggi daripada LOPW yang sepadan dan terdiri daripada konglomerat sebatian oksigen yang pukal dan bersifat reaktif. Walaubagaimanapun, pemangkin memudahkan tindak balas

sekunder, bagi menghasilkan minyak-bio yang mengandungi sebatian oksigen yang kecil dan stabil bagi kumpulan tertentu. Fenol, asid, benzena terbitan, ester antara lain yang membentuk sebatian kecil dan stabil dalam minyak-bio yang dipilih oleh pemangkin. Profil uraian dan kinetik pirolisis LOPW ditentukan melalui permeteran gravity haba. Thermograf dari analisis permeteran gravity haba menyimpulkan bahawa tindak balas pirolisis menguraikan LOPW melalui mod berperingkat. Analisis kinetik berdasarkan kaedah Coats-Redfern mendedahkan bahawa kinetik resapan dihuraikan dengan terbaik pada tahap kedua (tahap aktif) pirolisis haba dan bermangkin. Sementara, kinetik sekaitan geometri dihuraikan dengan terbaik pada peringkat kedua dan ketiga, sebaliknya kinetik berasaskan Avarami-Erofe'ev dan Hukum kuasa menggambarkan peringkat ketiga pirolisis LOPW. Dari parameter kinetik, pirolisis bermangkin menunjukkan tenaga pengaktifan yang paling rendah berbanding pirolisis haba yang sepadan. Oleh itu, pirolisis LOPW boleh dihuraikan dengan baik mengikut mekanisme berbilang langkah kompleks. Indeks ciri penguraian (D) untuk pirolisis campuran LOPW/ Fe/HAPAZ lebih tinggi daripada pirolisis LOPW. Indeks D mendedahkan bahawa Fe/HAPAZ sangat mempengaruhi pirolisis LOPW.

THERMAL AND CATALYTIC SLOW PYROLYSIS OF LIGNOCELLULOSIC OIL PALM WASTES USING ZEOLITE AND HYDROXYAPATITE BASED CATALYSTS

ABSTRACT

The concern associated with industrial wastes motivated the production quality bio-oils from pyrolysis of lignocellulosic oil palm wastes with viable mesoporous catalysts derived from waste steel-slag. This study investigated the thermal and catalytic pyrolysis of LOPW over zeolite and zeolite-hydroxyapatite based catalysts to produce quality bio-oils in a slow-heating fixed-bed reactor. Also, the kinetics of the thermal and catalytic pyrolysis of the LOPW was investigated by using the Coats-Redfern methods. The reactor was maintained at 450-600 ^{o}C pyrolysis temperatures, 200 mL/min N_2 flowrate, 10 ^{o}C/min heating rate and 0.5-2.5 g catalyst load was used for the catalytic pyrolysis. The pyrolysis was performed over zeolite and zeolite-hydroxyapatite, as catalysts prepared from electric arc furnace slag. The BET textural characteristics suggested that the catalysts are hierarchical and highly mesoporous with average pore diameter ranging from 23-25 nm. The zeolite catalyst has crystallite structure consistent with that of Faujasite-Ca zeolite, based on authentication by XRD analysis. Whereas, Faujasite-Ca zeolite and hydroxyapatite crystallite formed the composite structure of hydroxyapatite-zeolite-based catalysts. The thermal pyrolysis produced crude bio-oils (CBO) at maximum yield of 40-47 wt% under 500-550 ^{o}C pyrolysis temperatures, whereas, the catalytic pyrolysis over 0.5 g catalyst is 40-47 wt%. The CBO have high heating values from 21-24.68 MJ/kg higher than that of the corresponding LOPW and comprised of conglomerate of bulky and reactive oxygenated compounds. But, the catalysts facilitated secondary reactions, which produced bio-oils pervaded with small and stable oxygenated compounds of specific

families. The phenolics, acids, benzene derivative, esters among others constitute the light and stable compounds in the bio-oils that the catalysts were selective to. The decomposition profiles and kinetics of the pyrolysis of LOPW were determined via thermogravimetry. The thermographs from the thermogravimetric analysis inferred that pyrolysis reactions decomposed LOPW via stage-wise mode. The kinetics analysis based on the Coats-Redfern's methods revealed that diffusion kinetics best described the second stage (active stage) of thermal and catalytic pyrolysis. While, the geometrical correlation kinetics best described the second and third stages, conversely kinetics govern by Avarami-Erofe'ev and Power law described the third stages of the LOPW pyrolysis. From the kinetics parameters, the catalytic pyrolysis exhibited the lowest activation energies compared to the corresponding thermal pyrolysis. Therefore, the pyrolysis of LOPW can be best described to follow complex multi-step mechanisms. The characteristic decomposition index (D) for the pyrolysis of LOPW and Fe/HAPAZ blend were higher than those for the LOPW thermal pyrolysis. The index D revealed that the Fe/HAPAZ profoundly influences the LOPW thermal pyrolysis.

CHAPTER ONE
INTRODUCTION

1.1 Background

Fossil fuels provide the energy for transportation and industrial operations and several chemicals with accompanying environmental problems associated with global warming. Lignocellulosic biomass is carbon neutral, abundant and readily available to supplement the energy and chemicals demands, and also reduce carbon dioxide emission to mitigate global warming (Zhang et al., 2013). Biomass wastes are suitable for processing into valuable products for energy and chemicals. Attention shifted to using lignocellulosic oil palm wastes (LOPW) from oil palm mills as a potential precursor to renewable energy resources and chemicals synthesis.

Environmentally friendly chemical processes that enable resource recycling and utilization of industrial waste have recently attracted much attention. Practical processes for converting waste materials into useful materials contributes to solving the problems of the waste management. Thermochemical processes such as liquefaction and pyrolysis converts lignocellulose biomass to mainly bio-oil and other chemicals (Venderbosch and Prins, 2010). Liquefaction produced particularly bio-oils at low yield with high quality compared to those from pyrolysis. Focus shifted towards pyrolysis of lignocellulose biomass for high bio-oil yield at low-cost (No, 2014).

Lignocellulosic biomass from forest, agricultural and agroindustries are processed via pyrolysis to to bio-oils, biochar and gas. Depending on the desired product, the biomass can be thermally decomposed by pyrolysis at slow or fast heating rates. The slow-heating pyrolysis (slow pyrolysis) produces primarily biochar, the residual bio-oil and gas are rarely attended for any uses. Lignocellulosic biomass undergoes pyrolysis in several types of reactors. Beech wood, beech bark pellet, and babool seeds are pyrolyzed in a batch-fluidized reactor and in a fixed-bed reactor. The

pyrolysis decreases the oxygen and hydrogen content of the biochar and bio-oils, and their high heating values (HHVs) increase above those of the corresponding biomass (Garg et al., 2016; Morin et al., 2016). The pyrolysis reactions involve depolymerization, fragmentation and cracking of the cellulose, hemicellulose, and the lignin of the biomass (Li et al., 2017). The reactions create a unique composition of bio-oil based on the reactor conditions depending on the composition of the biomass. Heterogeneous and widely distributed compositions of stable oxygenated compounds characterized the resultant bio-oils.

The bio-oils have been extensively studied and classified by characterizations (Mohammed et al., 2016; Torri et al., 2016). The characterisation confirm the inherent chemical composition and physical properties of the bio-oils (Santos et al., 2015). The literature has reported the inherent features of several bio-oils derived from the pyrolysis of lignocellulosic biomass. The oxygenated compounds prevail in the bio-oils and militated against their HHVs (Alagu et al., 2015; Saikia et al., 2015). The HHVs of bio-oils ranged from 16.79 - 19 MJ/kg, higher than that of the corresponding biomass, close to that of oxygenated fuel such as ethanol and lower than 40 - 45 MJ/kg for fossil fuels.

Pyrolysis of biomass over various costly commercial and laboratory synthesized catalysts altered the composition of the bio-oils via reduction in oxygen, as CO_2, H_2O and CO. The resultant bio-oils would have less oxygenated compounds and water content than bio-oils from the corresponding thermal pyrolysis. Consequently, the fuels and fine chemical characteristics of the bio-oils improve to above those of the bio-oils of the corresponding thermal pyrolysis. Catalyst change the composition of vapors from thermal pyrolysis of lignocellulose biomass. Catalysts such as Zeolite (ZSM-5, HZSM-5 and Fluid catalytic cracking catalyts), and alkaline

(Na_2CO_3/γ-Al_2O_3, K_2CO_3, $Ca(OH)_2$ and MgO are often used during biomass pyrolysis, they influences the change in the bio-oils composition (Mullen et al., 2018). The catalysts change the bio-oil composition via cracking and deoxygenation reactions on the crude pyrolysis vapour (CPV) from thermally decomposed biomass by pyrolysis (Liang et al., 2018). Catalysts caused the thermally driven pyrolysis reactions to yield high quality bio-oil with more non-reactive oxygenated compounds (Marion et al., 2017). Scholars extensively discuss the main aspects of catalytic pyrolysis such as pyrolysis technology and processes, catalyst type activity and deactivation, parameters influence, biomass feedstock, and reaction mechanism. Previously, Akhtar & Saidina (2012) evaluated the influence of severity on zeolite catalysed biomass pyrolysis on the maximum yield of the desired bio-oil. Lappas et al. (2012) appraised the use of zeolite as catalyst during pyrolysis of lignocellulosic biomass for bio-oil production with few consideration to the use of base catalysts. Similarly, Rezaei et al. (2014) explained the catalytic activities of several zeolite as catalysts for the selective production of aromatics and olefins in biomass pyrolysis. Furthermore, Dickerson and Soria (2013) reported the effect of various catalyst over pyrolysis reaction with particular attention to reaction pathway and mechanism leading to the yield of the resultant bio-oil. However, Isahak et al. (2012) discussed on catalytic pyrolysis of biomass with focus on the type of pyrolysis reactor and conditions.

Hierarchical narrow pore network of the zeolite catalysts restricts traffic of the bulky molecules inside the pore structure. The bulky molecules decomposed causing coke agglomeration. The coke clogs the zeolite pores, which affect their catalytic activities. The resultant bio-oils have broad distribution of organic compounds like that of the thermal pyrolysis. Catalysts significantly influences product selectivity and distribution of bio-oil compounds (Junior et al., 2018). Varying pyrolysis conditions,

such as catalyst loading and temperature, they concurrently influence the yields and composition of bio-oils. Operating parameters are also tempered to direct the pyrolysis reactions to ultimately achieve the desired bio-oils yield and composition. The typical operating parameters for biomass pyrolysis studies include catalyst loading pattern, biomass particle size, nitrogen flowrate, pyrolysis temperature and reaction time (Bai et al., 2018).

Iron and steel industries produced large amount of solid residues such as basic oxygen furnace slag (BOFS) (Kuwahara et al., 2013) and electric arc furnace slag (EAFS) (Teo et al., 2014). The slags accumulated over a long period of operation cycles and constitute waste management problems and other relevant environmental issue. The primary components of the slags include CaO, SiO_2, $A1_2O_3$, MgO, Fe and little amount of transition metals oxides (Kuwahara et al., 2009; Nasuha et al., 2016). The compositions provided the slags with the leverage to be converted into valuable materials such as cheap adsorbents and catalysts to mitigate the waste management issues (Balakrishnan et al., 2011; Kar and Gurbuz, 2016; Kuwahara et al., 2013). The synthesis of cheap catalysts for the pyrolysis of lignocellulosic biomass can be an approach for the value-added utilization of the EAFS waste material. These catalysts faces the challenges of the industrial-scale application of biomass pyrolysis (Yildiz et al., 2016). The catalysts that can limit coke formation and char agglomeration can reduce the economic and technical difficulties in the industrial application. Additionally, catalyst loading be optimized to guarantee efficient contact between pyrolysis vapors and the active sites on the catalyst and ultimately achieve precise industrial application of pyrolysis.

1.2 Problem statement

In Malaysia, there is growing interest in the use of renewable resources such as lignocellulosic biomass in thermochemical conversion processes to produce biofuels and advanced materials, is among the primary motivations for this study.

Pyrolysis technologies process large quantity of lignocellulosic biomass wastes into to primarily biochar and activated carbon environmental remediation. The processes generated huge quantity of the residual bio-oils and often discarded. The quest is to utilize the bio-oils, as renewable waste resources to serve as precursors for renewable fuel and chemicals.

The heterogeneous bulky and reactive oxygenated compounds in broad composition affect the quality of the pyrolysis residual bio-oils. This promote the pursuit to upgrade the quality of the bio-oils with catalyst to high-grade precursor for the renewable fuels and chemicals. There is rising need for highly mesoporous catalysts to mitigate the drawbacks associated with the use of microporous catalysts during the pyrolysis of the lignocellulosic biomass. The microporous catalysts are shape selective, hinder the traffic of the bulky reactive molecules of crude pyrolysis vapour (CPV) inside the catalysts internal structure, which caused coke on the catalyst surface and encourages biochar agglomeration. The coke affects the catalyst activity during pyrolysis of biomass.

Electric arc furnace slag (EAFS), waste generated from steel scraps converted to steel in an arc furnace by using electric current. The annual production resulted in an apparent waste management and environmental issues. The importance in synthesizing low-cost advanced materials prompts the processing of the EAFS into catalysts for production of quality bio-oils from lignocellulosic biomass pyrolysis.

The contribution of this study is the synthesis of highly mesoporous and hierarchical mesoporous composite f hydroxyapatite-zeolite catalysts from rarely used precursor EAFS, a waste from metallurgical industry. The catalysts are expected to be active in catalytic pyrolysis lignocellulosic oil palm wastes.

1.3 Objectives of the study

The specific objectives of the study were:

1. To examine the pyrolysis of lignocellulosic oil palm wastes (LOPW) and determined the pyrolysis conditions that affect the composition and yield of the resultant bio-oils. The best conditions were down selected and used in catalytic pyrolysis studies.
2. To synthesize and characterize the highly mesoporous Faujasite-SL, hydroxyapatite-zeolite and Fe/ hydroxyapatite-zeolite catalysts prepared from electric arc furnace slag (EAFS).
3. To demonstrate the efficacy of the highly mesoporous zeolite and zeolites hydroxyapatite-based catalysts in permeating the resultant bio-oils obtained from thermally decomposed LOPW with light and stable oxygenated compounds.
4. To determine the kinetics and parameters that best describe the pyrolysis of LOPW over Fe/hydroxyapatite-zeolite catalyst by using kinetics of the Coats-Redfern's methods.

1.4 Scope of the study

The study involves the production of bio-oils from the thermal and catalytic pyrolysis of lignocellulosic oil palm waste (LOPW) on a slow-heating fixed-bed

reactor. The reactor conditions are set at pyrolysis temperature of 400-600 ^{o}C and heating rate of 10 ^{o}C and N_2 flowrate of 200 mL/min for the thermal and catalytic pyrolysis studies, while catalyst load of 0.5-2.5 g and biomass of 5.0 g were placed inside the reactor during the catalytic pyrolysis.

The EAFS is the primary feedstock for the synthesis of the catalysts for catalytic pyrolysis. The study includes synthesis of highly mesoporous zeolite and hydroxyapatite-based catalysts from EAFS. The catalysts activities would be studied in the pyrolysis of the LOPW at various temperatures and catalyst loading to reveal the selectivity of the catalysts based on the chromatographic compositions of the resultant bio-oils by GC-MS.

Thermogravimetric analyses would be conducted to establish the decomposition patterns and kinetics, and to ascertain the decomposition index of the biomass during thermal and catalytic pyrolysis.

1.5 Thesis organization

This thesis comprises of five chapters outlined in sequence to elucidated on the primary idea of the study. The summary of contents of each chapter are presented below:

Chapter one (introduction)

The chapter presented the overview on the environmental issue associated with the feedstocks for the catalyst synthesis, biomass precursor and fossil fuels. Also, the chapter highlights the use of biomass pyrolysis in the production of renewable materials for fuels and chemicals. The problem statement, research objectives, scope and organization of the thesis are also presented.

Chapter two (literature review)

The chapter present extensive review in the pyrolysis reactions pathways. It highlighted the challenges and unfulfilled gap in knowledge. Also, it reviewed previous studies on reaction conditions catalyst activities and kinetics to figure out drawbacks and gaps that requires improvement.

Chapter three (Materials and methods)

This chapter presents the materials, chemicals, equipments used for conducting the study. The procedure for catalyst synthesis, description of the pyrolysis procedures and characterisations of the catalyst, feedstocks and products for the pyrolysis studies are outlined in this chapter.

Chapter four (Results and discussion)

Chapter four presents the outcome of the various studies, interpretation and analysis of results obtained during the entire study. The chapter consist of three sections; the thermal pyrolysis, promotion of highly mesoporous zeolites and zeolite-hydroxyapatite for production of bio-oils from lignocellulosic oil palm wastes (LOPW) and Elucidating the thermal and catalytic decomposition of LOPW and determination of the biomass kinetics by using isoconversional model-free methods.

Chapter five (Conclusions and recommendations)

This chapter presents the primary research findings along with suggested recommendations on future studies in synthesis catalysts and upgrading the resultant bio-oils.

CHAPTER TWO

LITERATURE REVIEW

This literature review explores the role of catalysts in biomass pyrolysis for the production of quality bio-oils as precursors for fuels and chemicals. Major components and parameters related to the nature and compositions of lignocellulosic biomass are discussed. A brief review on the various catalysts used in some relevant and related studies are conducted, which are classified as microporous and mesoporous catalysts and metal modified catalyst. The various techniques of biomass pyrolysis are elucidated to highlight their potential regarding the thermochemical conversion of lignocellulosic biomass to quality bio-oils. The effect of catalyst and variant pyrolysis conditions on the yield and composition of the resultant bio-oils are discussed. Lastly, the kinetics of biomass decomposition by thermal and catalytic pyrolysis are reviewed.

2.1 Lignocellulosic biomass

2.1.1 Types and availability of lignocellulosic biomass wastes

Lignocellulosic biomass residues is, because of low cost and extensive availabiliy has been used as potential feedstocks for synthesis of renewable energy and biochemicals. Agro-industries operations generate many lignocellulosic biomass residues including rice husk, rice straw, sugarcane bagasse, and lignocellulosic oil palm wastes (LOPW). Ample availability of the residues and the continous development of biomass enegy conversion technology has turned these biomass into important source of renewable energy and chemicals.

In Malaysia, the oil palm industry is quoted as the main sector generating abundant biomass wastes as renewable sources; these include empty fruit bunches

(EFB), mesocarp fiber (MF), palm kernel shell (PKS), oil palm fronds (OPF)and oil palm trunks. About 95.38 Mt of empty fruit bunches (EFB) is processed based on the standard biomass to EFB extraction rate. The estimated oil palm biomass generated along its supply chain comprised 21.03 Mt of pruned OPF, 7.34 Mt of EFB, 4.46 Mt of PKS and 7.72 Mt of MF, in all totaling 40.55 Mt (Loh, 2017).

2.1.2 Composition of lignocellulosic biomass

Photosynthesis reaction synthesizes lignocellulosic biomass from water, atmospheric carbon dioxide and solar energy. Hemicellulose, cellulose and lignin in a complex matrix that formed the tissues and define the chemical component of lignocellulosic biomass. Depending on the biomass, carbohydrate (hemicellulose and cellulose) have the largest fraction than the lignin among biomass. The lignin and hemicellulose intimately enclosed the cellulose, isolating for conversion into individual glucose monomers is difficult via non-thermochemical process (Saini et al., 2014). The biomass have similar components irrespective of the plant species, but only vary in composition (Casoni et al., 2018). Typically lignocellulosic oil palm waste comprise of 25–50 wt% cellulose, 15–40 wt% hemicellulose, 10–40 wt% lignin, 0– 15 wt% extractives, and fraction of inorganic mineral matter (Awalludin et al., 2015; Kan et al., 2016). The lignin is central to the pyrolytic conversion of lignocellulosic biomass to bio-oil pervaded with phenolic compounds. Notably, the chemical compositions are consistent with numerous ones previously reported in the literature (Isahak et al., 2012; Saini et al., 2014).

Tables 2.1 shows that the lignocellulosic biomass contains a considerable quantity of cellulose, hemicellulose, and lignin at varying composition.

Table 2.1 Chemical compositions of lignocellulosic biomass.

Biomass	Structural composition (wt.%)			References
	Cellulose	Hemicellulose	Lignin	
Douglas fir	44	21	32	(Wang et al., 2018)
Sunflower seed hulls	39.10	18.40	20.40	(Casoni et al., 2018)
Perennial Grass (Saccharum ravannae L.)	30.10	34.70	22.90	(Saikia et al., 2018)
Castor residues	38.42	22.40	20.20	(Kaur et al., 2018)
Pine sawdust	55.92	15.35	10.55	(Mishra and Mohanty, 2018a)
Coffee ground residues	10.6	36.6	40.6	(Fermoso and Mašek, 2018)
Durian shell	13.01	60.45	15.45	(Tan et al., 2017)
Oil palm shells	30.40	32.50	53.90	(Romero Millán et al., 2017)
Coconut shells	12.70	20.50	13.50	(Romero Millán et al., 2017)
Bamboo guadua	49.80	36.50	25.10	(Romero Millán et al., 2017)
Napier grass	38.75	19.76	26.99	(Mohammed et al., 2017)
Camellia sinensis branches	35.31	19.15	27.80	(Zhou et al., 2017)
Chestnut shells	31.61	22.64	42.69	(Özsin and Pütün, 2017)
Cherry stones	26.96	26.88	42.16	(Özsin and Pütün, 2017)
Grape seeds	13.83	18.71	49.23	(Özsin and Pütün, 2017)
Palm kernel shell	20.8–27.7	21.6–22.3	44.0–50.7	(Chang et al., 2016)
Wheat straw	32.3–36.3	21.1–30.6	16.8–25.5	(Chang et al., 2016)
Pine sawdust	48.6–52.6	10.5–12.2	25.3–26.5	(Chang et al., 2016)
Mango seed shell	49.99	21.15	25.53	(Andrade et al., 2016)
Eremurus spectabilis	38.50	20.50	30.10	(Aysu, 2015)

2.1.3 Structure of lignocellulosic biomass

Cellulose is a crystalline biopolymer comprising of stable hydrogen-bonded chains of 1-4-βlinked glucose (Anca-couce, 2016; Mendu et al., 2011). Attribute to the crystalline structure, cellulose is thermally stable and difficult to deploymirized into individual glucose monomers units under low temperature. Figure 2.1 shows a typical structure of the cellulose, lignin and hemicellulose. The hemicellulose as an amorphous organic polymer, it comprises of carboxyl group easily decompose by thermochemical reaction such as pyrolysis at earlier temperatures than that of cellulose. Carboxyl group constitute the major functional group of the hemicellulose, whereas cellulose comprises of both carboxyl and carbonyl group (Huang et al., 2012).

Both the cellulose and hemicellulose degraded within a narrow temperature of 200 – 315 ^{o}C under pyrolysis conditions, but earlier than the lignin (Hadar, 2013). Typically, the primary hemicellulose in lignocellulosic biomass is xylan, formed from a backbone of ß-(1→4)-D-xylopyranose units (Shen et al., 2015). Hydroxyls and methoxy-substituted phenylpropane monomers formed the lignin structure as a complex branched amorphous polymer. Alcohols linked to aryl ether and carbon-carbon bonds formed the different types linkages of lignin structure. The strong bonds of the linkages, including β-O-4, α-O-4, 5-5, β-5, and β-β formed numerous section of the lignin chemical structure (Adhikari et al., 2014; Pandey and Kim, 2011). Therefore, the strong bond characterized thermal decomposition of lignin to occur over a broad range of temperature from about 150 – 900 ^{o}C during pyrolysis (Geng, 2013).

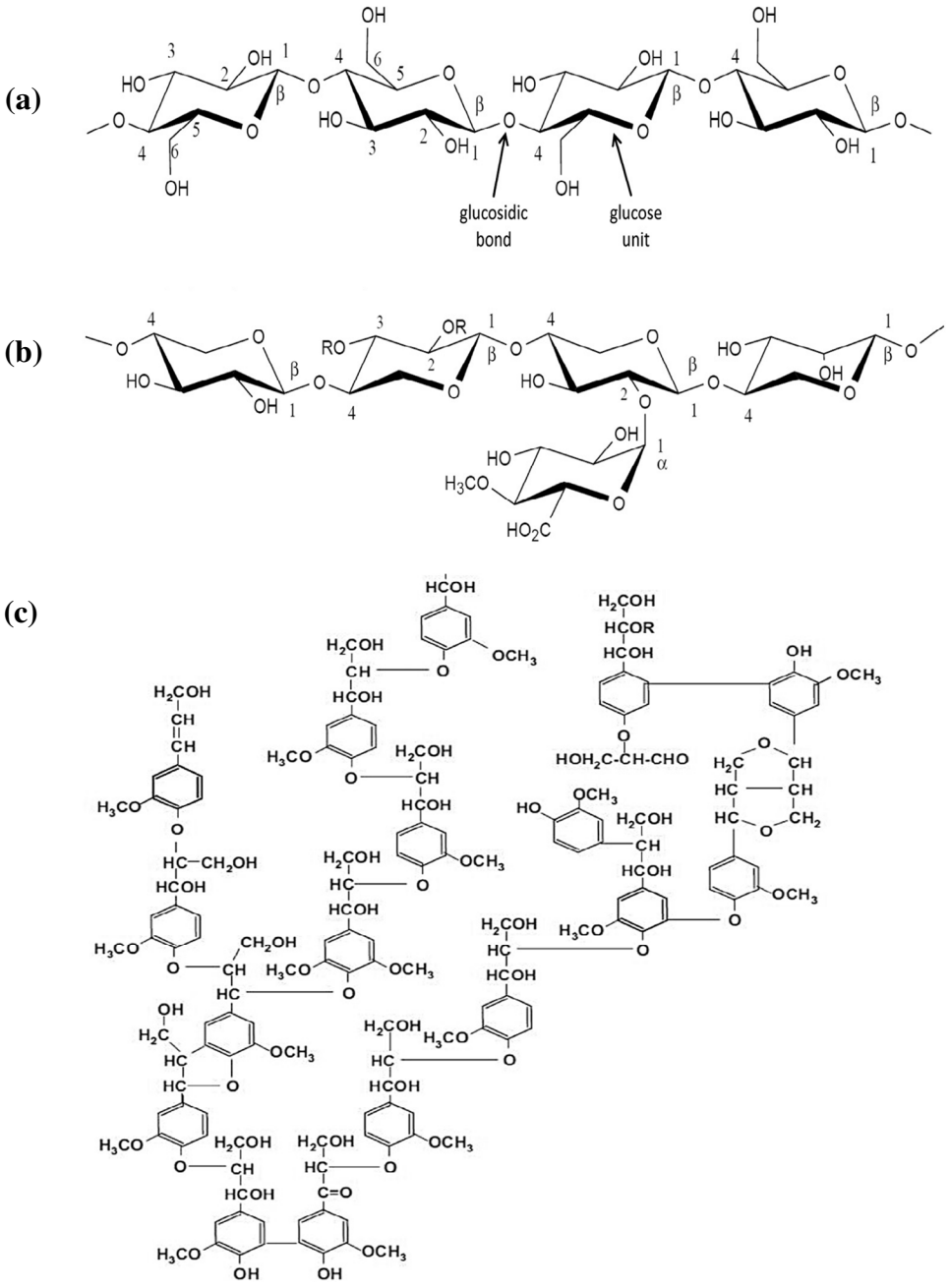

Figure 2.1 Typical structures of (a) cellulose, hemicellulose (xylan) and (c) lignin of lignocellulosic biomass (Anca-couce, 2016).

2.1.4 Lignocellulose biomass proximate and ultimate compositions

Quantitative techniques determine the composition and parameters that characterize lignocellulose biomass for thermochemical conversion. The techniques determine structural compositions, the proximate and elemental compositions and heating values of numerous lignocellulosic biomass (Mullen et al., 2018; Rajamohan and Kasimani, 2018). Tables 2.2 present the compositions of lignocellulose biomass from some domain pyrolysis studies for synthesis of high grade bio-oils. Numerous lignocellulosic biomass wastes are evaluated to establish their potential as feedstocks for synthesizing pyrolysis products such as bio-oils. Pyrolysis concedes the biomass to be devolatilized and become bio-oils and permanent gases leaving behind residual biochar. The biomass with low ash and with high volatile matter favors a high bio-oil yield (Mendu et al., 2011). The lignocellulosic biomass contains 36.89 – 59.5 wt% C, 4.40 – 8.57 wt% H, 23.46 – 48.24 wt% O. Whereas, the heating values range from 15 – 19.50 MJ/kg. The oxygen content is high, which characterize the lignocellulosic biomass with low heating values compared to fossil fuels. But, nitrogen, sulfur and ash contents are low compared to the amount in fossil fuels.

Table 2.2 Proximate and ultimate compositions of lignocellulosic biomass.

Biomass	Proximate analysis (wt.%)				Ultimate analysis (wt.%)					HHV (MJ/kg)	References
	Moisture	Volatile matter	Fixed Carbon	Ash	C	H	N	S	O		
Sawdust	6.85	80.90	11.06	1.19	44.71	1.48	4.20	0.28	49.73	12.19	(Fernandez et al., 2018)
Peach pits	5.70	79.10	13.90	1.30	52.01	5.90	2.32	1.88	36.89	21.39	(Fernandez et al., 2018)
Calophyllum inophyllum seed cake	3.56	72.61	21.10	2.73	43.80	6.30	3.1	0.70	45.90	18.80	(Rajamohan and Kasimani, 2018)
Castor residue	11.14	74.30	9.16	5.40	43.59	5.56	4.69	-	46.16	14.43	(Kaur et al., 2018)
Pine sawdust	6.09	78.03	12.16	2.07	50.30	6.00	0.69	-	42.99	18.44	(Mishra and Mohanty, 2018a)
Coffee ground residue	5.00	76.40	22.70	0.90	53.90	7.10	2.30	-	35.80	23.40	(Fermoso and Mašek, 2018)
Napier grass	-	81.51	16.74	1.75	51.61	6.01	0.99	0.32	41.07	18.05	(Mohammed et al., 2017)
Chestnut shells	10.17	65.55	23.08	1.20	48.14	5.47	0.60	-	45.79	-	(Özsin and Pütün, 2017)
Eucalyptus woodchips	9.70	74.70	23.5	1.83	51.23	5.93	0.13	0.00	42.71	20.04	(Hernando et al., 2017)
Camellia sinensis branches	7.24	79.00	11.92	1.84	44.74	3.49	1.01	0.12	48.93	13.83	(Zhou et al., 2017)
Oil palm shells	9.50	69.90	19.00	1.60	46.70	6.50	0.60	-	46.2	19.60	(Romero Millán et al., 2017)
Coconut shells	10.20	71.40	17.10	1.30	46.80	5.80	0.30	-	47.10	18.70	(Romero Millán et al., 2017)
Wheat straw	12.81	83.08	10.29	6.63	38.34	5.47	0.60	0.37	-	14.68	(Biswas et al., 2017)
Rice straw	11.69	78.07	6.93	15.00	36.07	5.20	0.64	0.26	-	14.87	(Biswas et al., 2017)
Palm kernel shell	-	75.21	22.74	2.05	50.73	5.97	0.36	0.06	40.83	20.35	(Chang et al., 2016)

2.2 Pyrolysis of lignocellulose biomass

Pyrolysis embroils thermal degradation of lignocellulose biomass through a sequence of complex reactions in an oxygen free environment, mostly created by sweeping Nitrogen gas. The biomass structural components decompose to lower molecular weight products such as bio-oil, gas and biochar. The products featured as sources of renewable energy and chemicals.

2.2.1 Advantages of pyrolysis

Pyrolysis technique gains a vast adaptability because it's operating parameters can be optimized to achieve the desired results. High yield of biochar can be achieved at low heating rate under slow pyrolysis, while high bio-oil yield comes via high heating rate fast pyrolysis. The technique received credence as a tool for biomass waste conversion to value added products such bio-oil, permanent gases and biochar (Abnisa et al., 2013; Biswas et al., 2017; Oh et al., 2016). The products are nurtured with low sulfur and nitrogen, which make them environment friendly (Mishra and Mohanty, 2018a). The overwhelming advantages of pyrolysis is that, it is less complex, and flexible to feedstock type and operating conditions (Yu et al., 2017). Most dry, wet, hard and soft biomass, sewage sludge and other industrial waste can be treated via pyrolysis without much difficulty. Often, the pretreated feedstocks enhanced performance of the process and product qualities. Therefore, tuning the conditions can produce products with characteristics of the required specification (Tripathi et al., 2016).

2.2.2 Pyrolysis technology

Pyrolysis is an advanced technology that received attention because of the growing interest in the production of liquid fuel from lignocellulosic biomass. Pyrolysis degrade the biomass in inert environment and produce bio-oils, carbon-rich solid called biochar and gas. The cellulose, hemicellulose and lignin (Yu et al., 2017), as the primary component of lignocellulosic biomass decompose concurrently by depolymerization, within temperature ranges of 300–800 °C to produce the primary products. As an endothermic reaction, the heat required for the pyrolysis of several biomass ranges from 207-434 kJ/kg (Dhyani and Bhaskar, 2017).

The heat caused biomass to devolatilize to organic vapor comprising of oxygenated compounds derived from the decomposition of the biomass cellulose, hemicellulose and lignin (Salema and Ani, 2011). The vapors can be condensed to organic liquid, known as bio-oil and the non-condensable gas comprising of CO_2, CO, H_2, and CH_4 leave the pyrolysis reaction zone, while the carbon-rich residual is left behind as biochar (Rajamohan and Kasimani, 2018).

Pyrolysis technologies are classified into slow, intermediate, fast and flash pyrolysis and their characteristic parameters are shown in Table 2.3. The slow and fast pyrolysis are the most commonly used processes for the synthesis of bio-oil and biochar.

2.2.2(a) Slow pyrolysis

Slow pyrolysis is the conventional process for producing primarily biochar, and residual bio-oil and gas by using a lower heating rate and long residence time under temperatures ranging from 300–600 °C (Keey et al., 2018). In slow pyrolysis,

Table 2.3 Pyrolysis conditions and product distributions (Roy and Dias, 2017; Tripathi et al., 2016; Zeng et al., 2017).

Conditions	**Pyrolysis process**			
	Slow	Intermediate	Fast	Flash
Residence time (s)	300–550	0.5–20	0.5–10 s	<1 s
Heating rate (°C/s)	0.1–1.0	1.0–10 °C/s	10-200	~1000
Temperature (°C)	300–600	300–600	300–1000	300–1000
Particle size (mm)	5–50	1–5	<1	<0.5
Pressure (MPa)	0.1	0.1	0.1	0.1
Products	**Yields (wt%)**			
Bio-oil	<50	<75	20	20
Biochar	<35	<25	<20	<20
Gas	<40	<20	<75	<75

biochar and bio-oil yields depend on the feedstock properties and operating temperatures, and heating rate showed considerable effect on their yields. Therefore, the desirable nature of products can be achieved by tuning the process conditions to optimum values. The pyrolysis requires efficient heat transfer across the diameter of the biomass particle.

The biomass is heated at moderate temperatures (300-600 °C) for long residence times, typically for 5-30 min. The pyrolysis reactions under carefully controlled conditions can maximize the bio-oil yield. A bio-oil yield of above 40 wt% has been reported for the pyrolysis of deodar (Krishna et al., 2016) whereas, the yield for eastern redcedar woods is below 40 wt% (Yang et al., 2016). Long duration, heat and mass transfer limitations, and transition phenomena governs the progress of slow pyrolysis in nurturing the final products.

2.2.2(b) Fast pyrolysis

Fast pyrolysis optimizes the quantity and quality of bio-oil compared to slow pyrolysis (Roy and Dias, 2017; Yang et al., 2016). The pyrolysis involves

decomposing biomass to mainly bio-oil at a very high heating rate for a very short residence time. Several studies showed that the pyrolysis produces the maximum amount of bio-oil at pyrolysis temperature around 500-550 °C. Like slow pyrolysis, the fast pyrolysis conditions affect the biochar and gas yield, the gas yield increases as biochar and bio-oil yield decreases. The bio-oil yield depends on biomass characteristics and pyrolysis conditions. Fast pyrolysis prevents secondary cracking of the pyrolysis products to gas, therefore, careful control of reactions conditions results in high bio-oil yields (Yildiz et al., 2016).

The product distribution of the bio-oil from the various pyrolysis technology primarily depends on the composition of the biomass. Yu et al. (2017) investigated the pyrolysis characteristics of cellulose, hemicellulose, and lignin individually. It was observed that the decomposition of hemicellulose occurred at 220-315 ^{o}C. Cellulose decomposed in the temperature range of 314-400 ^{o}C. The decomposition of lignin took place in a wide range of temperature from 160-900 ^{o}C, generating highest solid residue (40 wt%) (Dhyani and Bhaskar, 2017).

2.2.3 Thermal pyrolysis of lignocellulosic biomass

Pyrolysis decompose the biomass components by depolymerization, defragmentation, cracking, dehydration and rearrangement reactions. In addition, other secondary reactions produce biochar and primary vapor comprising of non-condensable gases and organic fraction laden with bulky and reactive oxygenated compounds that can be processed into light and stable compounds. Particularly cellulose decomposed by endothermic reaction, whereas exothermic reaction governs the decomposition of hemicellulose and lignin.

The cellulose and hemicellulose contribute to the yield of carbonyl compounds (particularly acids) in the organic fraction of the volatile, and heterocyclic compounds such as furan derivatives (Shen et al., 2015; S. Wang et al., 2017a). Typically, lignin made of aromatic rings decomposed to organic volatiles laden with phenolic compounds such as guaiacoal, 4-methylguaiacol, 4- vinylguaiacol and vanillin. Also, syringol compounds such as 4-methyl- syringol and syringaldehyde occurred as fraction of the volatiles from the lignin pyrolysis (Shen et al., 2015). The aromatic compounds are often classified into several groups such as guaiacol, syringol, phenol and catechol groups. The classification is based on the number of $–OCH_3$ and –OH functional groups attached to a benzene ring. Figure 2.2. shows typical oxygenated compounds generally found in a typical pyrolysis vapor from pyrolysis decomposed lignocellulosic biomass.

The non-condensable gases released from biomass pyrolysis include CO_2, CO, CH_4 and other hydrocarbons (Sabegh et al., 2018). The hemicellulose decomposes causing a high CO_2 yield, whereas cellulose produced a high CO yield. The presences of aromatic ring and methoxyl, the lignin degrades releasing high amount of H_2 and CH_4 (Collard and Blin, 2014).

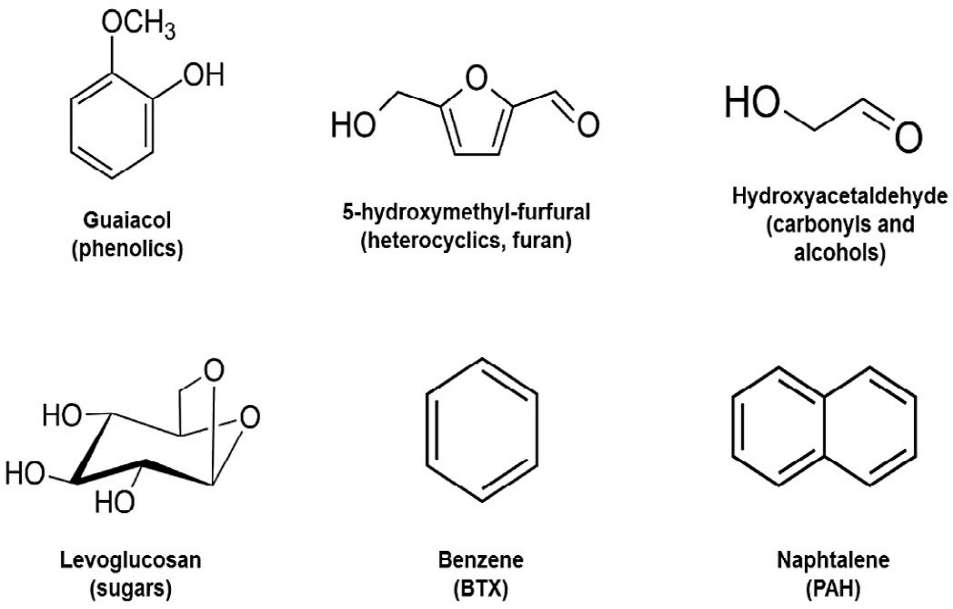

Figure 2.2 Representative compounds of vapor from lignocellulosic biomass pyrolysis (Anca-couce, 2016).

2.2.4 Mechanisms of pyrolysis of lignocellulosic biomass

2.2.4(a) Mechanism of cellulose pyrolysis

Figure 2.3 shows a typical cellulose decomposition mechanism via pyrolysis. Initially, pyrolysis transforms cellulose to either active cellulose that has a low degree of polymerization or turns into char and water. The active cellulose decomposes via

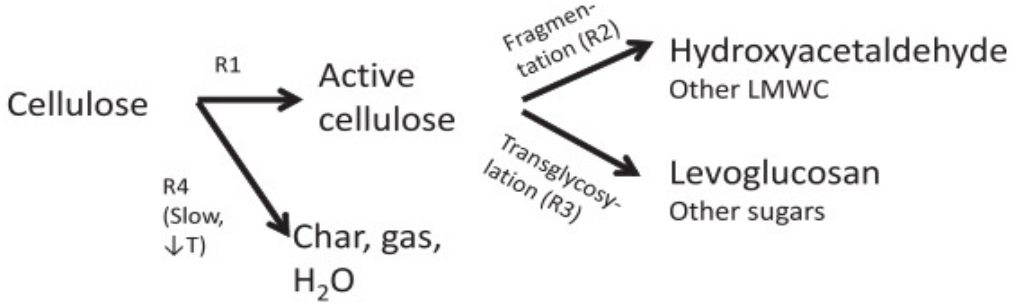

Figure 2.3 Reaction pathways cellulose decomposition by pyrolysis (Anca-couce, 2016).

two dissimilar pathways, cleavage of the glycosidic bonds to form levoglucosan, other anhydrosugars, cellobiose and higher sugar oligomers. The defragmentation characterizes the second pathway, which causes ring opens and breaks down into oxygenated compounds such as hydroxy acetaldehyde, formaldehyde, acetol, methylglyoxal and glyoxal (Wu et al., 2016). Also, hybrid reaction mechanism (competitive and consecutive) between levoglucosan and the low molecular weight fragments of furan derivatives, hydroxyacetaldehyde and acetol occurred to some extent during the cellulose pyrolysis.

At high temperature, rapid cleavage of the glycosidic bonds favor high volatile yield. The levoglucosan prevails as the primary compound at 400 ^{o}C and decrease as the temperature exceeds 530 ^{o}C. A notable decrease in the levoglucosan yield happens around 600 ^{o}C (Anca-couce, 2016). The secondary reactions contribute to the yield of carbonyl compounds in the resultant bio-oils, and heterocyclic compounds such as furan and furan derivatives (Zhang et al., 2015).

2.2.4(b) Mechanism of xylan-based hemicellulose pyrolysis

Thermal pyrolysis on xylan (model compounds) based hemicellulose such as α-D-xylose and several xylopyranosides produce compounds such as acetic acid, glycolaldehyde, furfural and 1:4-anhydroxylopyronose (Zhang et al., 2015). The reaction pathways for the primary and secondary decomposition of the monomeric units such as O-acetyl-4-O-ethylglucurono-xylan (including the xylan unit, O-acetyl xylan unit and 4-O-methylglucuronic acid unit) involve cleavage of the glycosidic linkage of the xylan chain and rearrangement of the depolymerized molecules respectively. A typical ring-opening reaction of the depolymerized xylan unit through the cleavage of the hemiacetal bond, followed by the dehydration between the

hydroxyl groups resulted to furfural. While, the prevalent mechanism is the primary elimination reaction of the active O-acetyl groups linked to the main xylan chain produced acids, typical of acetic acid.

2.2.4(c) Mechanism of lignin pyrolysis

Lignin as the most thermally stable component of lignocellulosic biomass, it decomposed over wide temperature range and consecutive reactions stages. Figure 2.4 shows the lignin degradation by pyrolysis to primary products via intermediate and secondary reactions. During the initial pyrolysis from 160–190 °C of pyrolysis temperature, the lignin softens followed by dehydration reactions at about 200 °C. The cleavage of α- and β-arylalkyl-ether linkages of the lignin happens from150-300 °C, aliphatic side chains cleavage occurs at about 300 °C, C—C linkages cleavage of occur from 370–400 °C and cleavage of methoxyl groups take place at about 310-340 °C for lignocellulosic biomass (Wang et al., 2017a). Secondary reactions produce phenolic compounds, water, carbonyls and alcohols and gas, such CO, CO_2 and CH_4. The phenolics prevail as the primary compounds of the volatiles fraction from lignin pyrolysis (Custodis et al., 2015; Yaman et al., 2018). The CH_4 and methanol are produced in high quantities from scission of methoxyl. The extra methoxy group in syringil units leads to increasing the CO_2, CH_4 and char yields.

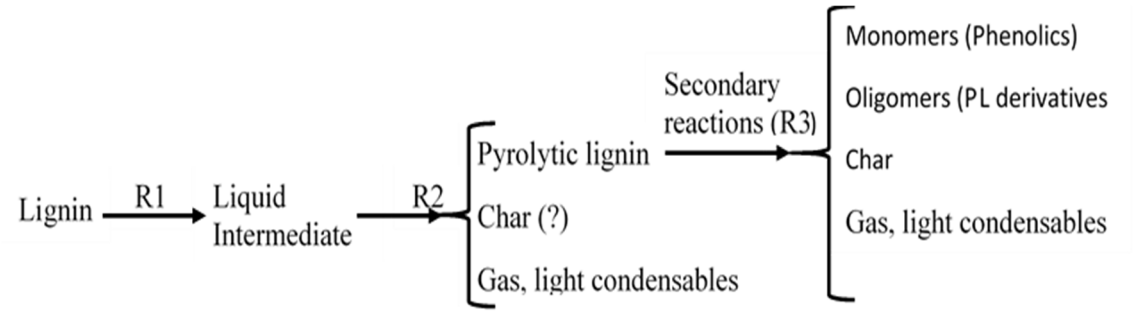

Figure 2.4 Reaction pathways for lignin decomposition by pyrolysis (Anca-couce, 2016).

Table 2.4 summaries the primary products obtained via pyrolysis mechanisms during the conversion of biomass components. Regardless of lignocellulosic biomass varying composition of lignin, cellulose and hemicelluloses, these organic polymers decompose via superposition of three main pathways namely, char formation, depolymerization and fragmentation and other secondary reactions.

Table 2.4 Compounds from primary decomposition of lignocellulosic biomass by pyrolysis (Collard and Blin, 2014).

Biomass constituents	Biochar formation		Depolymerization	Fragmentation
	T< 400 ºC	T> 500 ºC		
Lignin	-	CO, CH_4, H_2	Guaiacol, catechol, cresol, phenol	Formaldehyde, CO, CO_2, acetic acid, CH_3OH, CH_4
Cellulose	H_2O, CO_2	CO, CH_4, H_2	LG, 5-HMF, furfural	CO, CO_2, HAA, HA, AA
Hemicellulose				
Xylan	H_2O, CO_2	CO, CH_4, H_2	Furfural	CO_2, acetic acid, CH_3OH, formic acid, CO, HAA, HA
Glucomannan	H_2O, CO_2	CO, CH_4, H_2	LG, levomannosan, furfural	CO_2, acetic acid, CO, HAA, HA

LG: levoglucosan, 5-HMF: 5-hydroxymethylfurfural, HAA: hydroxyacetaldehyde, HA: hydroxyacetone, and AA: acetaldehyde.